COMPDYN 2019
7th ECCOMAS Thematic Conference on
Computational Methods in Structural Dynamics and Earthquake Engineering
M. Papadrakakis, M. Fragiadakis (eds.)
Crete, Greece, 24–26 June 2019

PRIOR IN-PLANE DAMAGE ON THE OUT-OF-PLANE RESPONSE OF MASONRY INFILLS

F. Akhoundi[1], **G. Vasconcelos**[2]

[1] Assistant Prof. Tabriz Islamic Art University
f.akhoundi@tabriziau.ac.ir

[2] Assistant Prof. University of Minho
graca@civil.uminho.pt

Abstract

Although the masonry infills are assumed as non-structural elements, their vulnerability during past earthquakes resulted in huge economical costs and life losses. The out-of-plane collapse of the infills is assumed as a common collapse mechanism. One important parameter on the out-of-plane collapse of the infills, is a presence of prior in-plane damage which in the present paper will be studied in detail.
In this scope, the main objective of this study is to analyze the out-of-plane experimental behavior of masonry infilled frames that are characteristic of Portuguese buildings and can be seen in other south European countries. In the experimental program, four half-scale specimens were constructed; one reference specimen and three specimens with different prior in-plane damage related to the in-plane drifts of 0.3%, 0.5% and 1%. The out-of-plane loading was applied uniformly to the brick infills by means of an airbag to simulate the effect of earthquakes. The results show that presence of prior in-plane damage affects the out-of-plane response of the specimens and a formula was derived to predict the out-of-plane stiffness and resistance of the infills taking into account the effects of prior in-plane damage.

Keywords: Masonry Infills, Prior In-Plane Drift, Out-of-Plane.

1 INTRODUCTION

The relevance of studying the out-of-plane behavior of brick infill walls was brought to light in the recent earthquakes occurred in Europe such as L'Aquila earthquake in 2011 [1], where severe damages developed in the infill walls in comparison to some minor cracks observed in the surrounding structure. In spite of the out-of-plane behavior of masonry infilled frames have attracted less attention from the research community than masonry infill under in-plane loading, some studies on the out-of-plane behavior of masonry infilled rc frames can be found in literature [2-4].

From experimental analysis, it has been observed that the masonry infill panel surrounded by rc or steel frame can resist significant out-of-plane loads due to formation of arching mechanism [4]. The development of the arching mechanism in the masonry infill is dependent on its confinement by the surrounding frame. When there is no confinement, the out-of-plane resistance is controlled by the rocking resistance along its base.

Arching mechanism within the infill may develop in horizontal, vertical or in both horizontal and vertical directions. When only horizontal or vertical arching mechanism develops, it means that the masonry infill has no proper confinement in its vertical or horizontal interfaces respectively. When all the interfaces between infill and frame provide confinement to the infill, both horizontal and vertical arching mechanism develops.

The effect of different boundary conditions on the out-of-plane behavior of the infilled frames was investigated by other researchers [3, 5, 6]. Different connecting conditions at the top interface between the infill and the frame were considered: (1) joint completely filled with mortar; (2) joint partially filled with mortar; (3) joint with a horizontal gap of 3 mm due to shrinkage of the fresh mortar and (4) masonry infill with unsupported top. No significant differences in the behavior of the infills with complete and partially filled top joint have been found. In case of the gap with 3 mm thickness in the upper mortar joint a clearly modified behavior of the specimen was recorded. The presence of an initial gap in the top joints increases the relative displacement in the gap causing tilting of the infill panel. Infill panel with unsupported top behaved as cantilever beam.

The experimental program carried out by Dawe and Seah [7] included 9 full scale masonry infilled steel frames subjected to uniformly distributed lateral pressure applied in small increments. The influence of boundary conditions, joint reinforcement, panel thickness and presence of openings was investigated. From the experimental results, it was concluded that infill compressive strength, panel dimension, boundary conditions and rigidity of the surrounding frame have a significant effect on the ultimate load. It was concluded that the infill having four supports at its boundaries without any slippage at them, represents higher out-of-plane resistance. It was also concluded that the ultimate load increases parabolically with increasing panel thickness, but decreases with increasing panel length and height. Parametric study was conducted and empirical equations for the prediction of the out-of-plane resistance, corresponding to different boundary conditions were represented. An extensive study about the influence of openings in the in-plane behavior of the infills was also studied in [8].

A series of experiments were performed by Angel et al [9] focusing on the out-of-plane resistance of masonry infill walls. The panels varied from uncracked specimens, cracked specimens and repaired specimens, to specimens tested with loads applied in both the in-plane and the out-of-plane directions. The tests were performed monotonically by means of an airbag in pressure control until the maximum allowable capacity of the system was reached. It was concluded that the in-plane cracking reduces the out-of-plane capacity of slender panels by a factor as high as 2 and the out-of-plane capacity of the panels is totally dependent on its

slenderness ratio and compressive strength. It was also concluded that the repairing techniques increased the out-of-plane capacity of damaged infills by a factor of 5.
Following the need to better understand the seismic behavior of existing brick masonry infills enclosed in rc frame buildings built in Portugal in the last decades, an experimental campaign was designed to analyze the out-of-plane behavior of traditional brick masonry infills. This paper presents and discusses the experimental results of the experimental campaign. Different parameters that are expected to influence the out-of-plan behavior were considered, namely the workmanship, central openings and previous in-plane damage. It should be mentioned that traditional brick infill walls that were built in recent past decades can be representative of brick infills in other south European countries, which point out also the relevance of the present work.

2 EXPERIMENTAL PROGRAM

In order to investigate the out-of-plane response of brick masonry infills within reinforced concrete rc buildings built in past decades in Portugal (in the 1980s) that are also representative of brick infills built in other south European countries, an experimental campaign was designed based on static out-of-plane tests. Six reduced-scale specimens were tested in the out-of-plane direction by applying uniform quasi-static out-of-plane loading. As the cavity walls were usually built without any ties between internal and external leaves, there is no interconnection between the leaves. In addition, the outer leaf of the cavity wall collapse much more often when compared to the internal leaf [1]. These reasons justified the application of the out-of-plane loading in the external leaf in the experimental tests.
In the experimental campaign, different variables were considered, namely: (a) workmanship quality; (b) presence of openings; (c) previous in-plane damage. The need of a new mason for the construction of the remaining specimens was derived from the poor workmanship used in the construction of one of the specimens. In case of prior in-plane damage, double leaf masonry infills were tested in the in-plane direction until a selected lateral drift. After the in-plane test, the internal leaf was removed and the out-of-plane load was only applied on the external leaf.

2.1 Characterization of prototype and designing reduced scale specimens

The prototype of an rc frame with masonry infills was defined based on a study carried out to characterize typical rc buildings constructed in Portugal since 1960s [10]. About 80 buildings were analyzed to identify cross sections of beams and columns, reinforcing schemes of those elements, geometry of brick masonry walls and the number, typology and position of openings within the walls. From this study, a prototype of a rc frame was defined having a length of 4.50m and a height of 2.70m. The cross section of rc columns was 0.3m x 0.3m (length x height) and of rc beams was 0.3m x 0.5m. The masonry infills were mostly built as cavity walls composed of two leaves with horizontal perforated brick units. The external leaf has mostly a thickness of 15cm and the internal leaf has typically a thickness of 11 cm, being both leaves separated by an air cavity of about 4 cm.
To overcome the space limitation in the laboratory and make handling of specimens easier, reduced scale rc frames were adopted in the experimental campaign. Reduced-scale specimens were designed following an allowable stress design approach. For the design of reduced scale specimens, an allowable stress design approach was followed. A scale factor of 0.54 was adopted to scale all elements, including the dimensions of the bricks. The reduced scale bricks were selected in a way among the factories' products to have similar perforation percentage with prototype. In the first step, the sections of the real scale rc columns and beams of the rc

frame prototype were analyzed based on ACI 318-08 [11] guidelines in order to obtain the maximum resisting forces and flexural moments in the columns and beams. After this, Cauchy's similitude law (Table 1) was applied to calculate the maximum allowable forces and bending moments of reduced scale cross sections from the maximum allowable forces and flexural moments of real scale sections obtained in the first step. Finally, cross-sections and reinforcement of the reduced scale structural elements were designed based on the same allowable stress design approach.

An overview of the scaled geometry and reinforcement scheme of the rc frame, as well as of the cross sections of columns and beams is shown in Figure 1 and Figure 2. For the masonry infills, horizontally perforated bricks of 175mm x 115mm x 60mm (length x height x thickness) and of 175mm x 115mm x 80mm were adopted for the internal and external leaves respectively. The reinforcement steel used for the construction of rc frame was of class A400NR, with a yielding tensile strength of 400MPa and for the concrete, a C20/35 class was adopted.

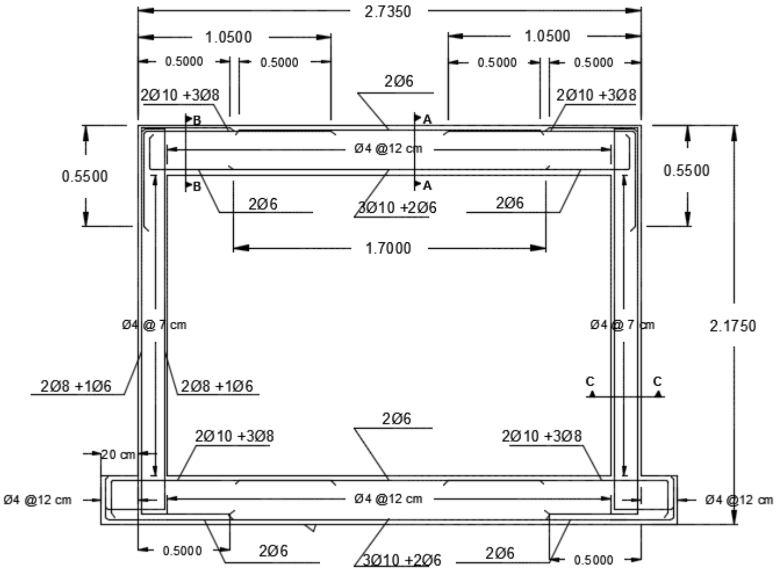

Figure 1. Geometry and reinforcement scheme of the reduced scale rc frame

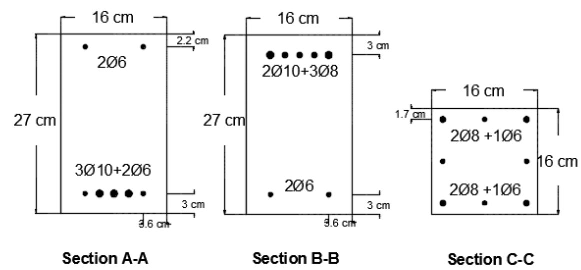

Figure 2. Cross-sections of columns and beams in reduced scale rc frames

The description of masonry infilled rc frames tested in the out-of-plane direction is given in Table 2. A reference specimen was tested to investigate the out-of-plane response of the brick masonry infill without any initial damage. Three specimens were also tested in the out-of-plane direction, after development of prior in-plane damage corresponding to different in-plane lateral drift levels of 0.3%, 0.5% and 1%. All these specimens were built by mason B. As leaves of the cavity infill wall are not connected and also based on the information provided earlier, it was decided to remove the internal leaf and apply the out-of-plane load in the previously damaged external leaf. This enables also to compare directly the results between damaged and non-damaged infill walls.

Parameter	Scale Factor	Parameter	Scale Factor
Length (L)	$\frac{L_P}{L_m}=\lambda$	Mass (m)	$\frac{m_P}{m_m}=\lambda^3$
Elasticity Modulus (E)	$\frac{E_P}{E_m}=1$	Weight (W)	$\frac{W_P}{W_m}=\lambda^3$
Specific Mass (ρ)	$\frac{\rho_P}{\rho_m}=1$	Force (F)	$\frac{F_P}{F_m}=\lambda^2$
Area (A)	$\frac{A_P}{A_m}=\lambda^2$	Flexural Moment (M)	$\frac{M_P}{M_m}=\lambda^3$
Volume (V)	$\frac{V_P}{V_m}=\lambda^3$	Stress (σ)	$\frac{\sigma_P}{\sigma_m}=1$
Displacement (d)	$\frac{d_P}{d_m}=\lambda$	Strain (ε)	$\frac{\varepsilon_P}{\varepsilon_m}=1$
Velocity (v)	$\frac{v_P}{v_m}=1$	Time (t)	$\frac{t_P}{t_m}=\lambda$
Acceleration (a)	$\frac{a_P}{a_m}=\lambda^{-1}$	Frequency (f)	$\frac{f_P}{f_m}=\lambda^{-1}$

Table 1. Relation between different parameters of prototype and model based on Cauchy's Similitude Law

Specimen	Masonry in-fill	Prior damage	Number of leaves during construction	Mason
SIF-O-1L-B	Solid	None	One leaf	B
SIF-IO(0.3%)-2L(NC)-B	Solid	Prior in-plane damage - drift of 0.3%	Double leaf with no connection	B
SIF-IO(0.5%)-2L(NC)-B	Solid	Prior in-plane damage - drift of 0.5%	Double leaf with no connection	B
SIF-IO(1%)-2L(NC)-B	Solid	Prior in-plane damage - drift of 1%	Double leaf with no connection	B

Table 2. Designation of the specimens tested under out-of-plane loading

2.2 Test Setup

The test setup designed for out-of-plane tests is shown in Figure 3. The bottom beam of the rc frame was attached to two steel beams (HEB300) that were instead attached to the reaction floor in order to avoid any sliding and uplifting. Additionally, the sliding of the rc frame with respect to those steel beams of HEB300 was prevented by bolting an L-shape steel profile (L200mm x 200mm x 20mm) to the steel beams, see Figure 3. In turn, the uplifting of the rc frame was prevented by bolting tubular steel profiles (two welded UNP140 steel profiles) to the steel beams. The out-of-plane movement at the top rc beam was restrained by attaching L-shaped steel profiles (L100mm x 100mm x 10mm) at each side of the upper concrete beam, which instead were bolted to the top steel frame, see Figure 4. Three rollers were placed on the L-shaped profiles to minimize or even eliminate the friction between them and the upper reinforced concrete beam during in-plane loading. To improve the robustness of top boundary restraint under out-of-plane loading, four steel rods M40 were attached to a steel triangular steel structure, connected to two HEB 240 steel profiles that were attached to the lateral reaction wall, see Figure 4.

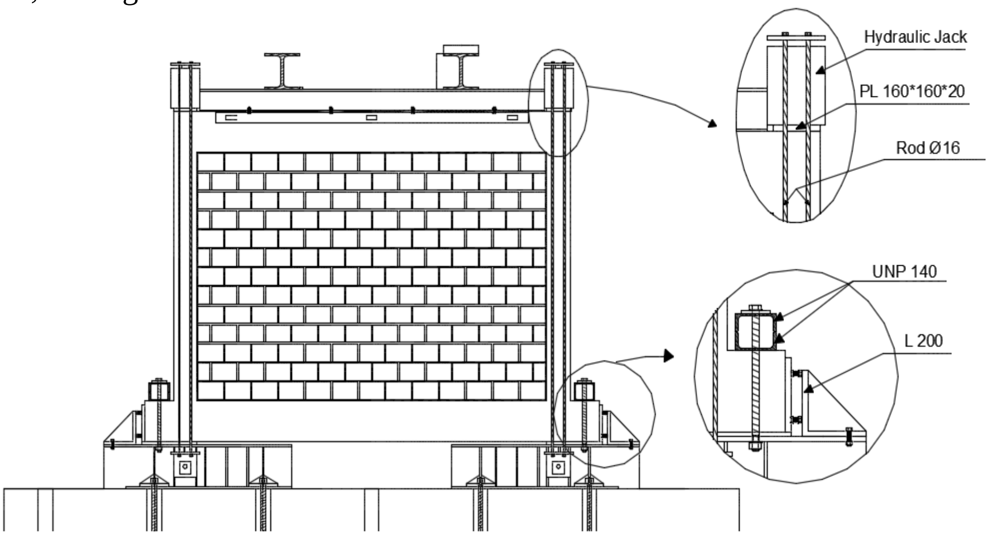

Figure 3. Test setup for out-of-plane testing

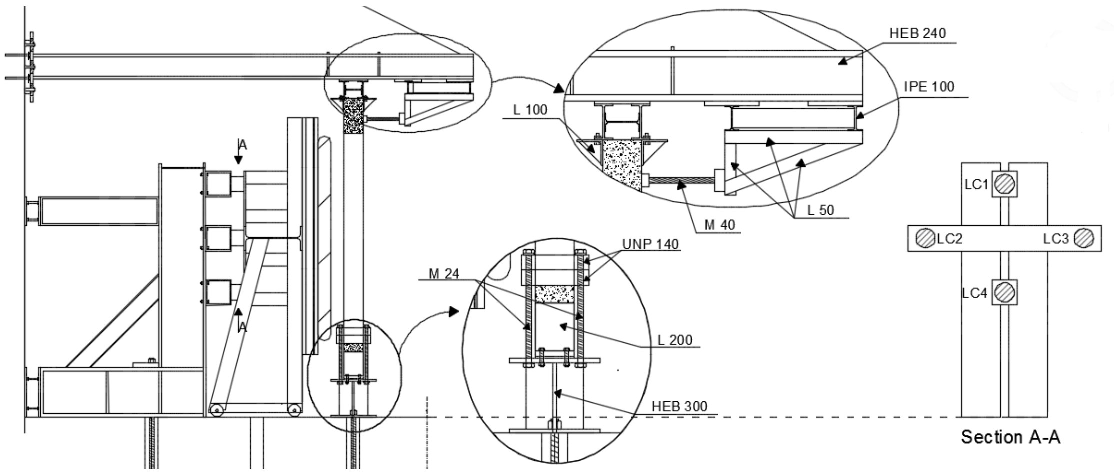

Figure 4. Test setup for out-of-plane testing

Two vertical jacks were placed at top of the columns to apply a vertical load of 160 kN, corresponding to 40% of the column's axial force capacity. Each jack was pinned to the lower steel beam by means of four vertical rods with a diameter of 16 mm (two at each side).

The out-of-plane loading was applied by means of an airbag installed between the masonry infill and a stiff wooden sandwich panel that was attached to a L-shaped reaction steel structure composed of HEB360 steel profiles. This structure was connected to the lateral reaction wall and to the reaction floor to completely prevent uplifting and sliding during the test. The L-shaped steel structure is stiffened at the top with a horizontal HEB220 steel profile and with inclined HEB160 steel profile. The stiff wooden sandwich panel is connected to the L shape steel structure by means of four load cells aiming at measuring the force applied by the airbag to the brick infill wall. The configuration of the load cells is presented in Figure 4(section A-A). Four rollers were added at the bottom part of the stiff wooden sandwich panel to enable its mobility along the horizontal direction without any friction, which could result in additional forces applied by the airbag. In case of the brick infill with a central opening, an airbag with adjusted geometry was used to correctly apply the out-of-plane load.

2.3 Instrumentation and loading pattern

The instrumentation plan is defined to record the most important displacements in the brick masonry infill walls with and without central opening subjected to out-of-plane loading and is shown in Figure 5.

The deformation of the brick infill, as well as the cracking propagation, was monitored in the free surface of the wall in front to the surface where the airbag was in contact with. To capture relevant out-of-plane deformations of solid brick infills, fifteen LVDTs were placed on the specimen according to the configuration shown in Figure 5a: (1) LVDTs 1 to 9 recorded the displacement of the infill panel at different locations (L1 to L9). This configuration enables to define deformation contour levels of the brick infills at different stages of loading; (2) LVDTs 10 to 13 measured the possible detachment of the masonry infill from the surrounding rc frame; (3) two additional LVDTs were placed to record possible out-of-plane movement of bottom and top rc beams (L14 and L15). The displacement recorded in these LVDTs should practically zero if the rc beams are adequately restrained to move in the out-of-plane directions. Therefore, these LVDTs are intended to control the suitability of the boundary conditions. In case of brick infill with central opening, 16 LVDTs were used to measure out-of-plane deformations during the test, see Figure 5b: (1) LVDTs 1 to 10 recorded the relevant out-of-plane deformations of the infill panel during loading (L1 to L10); (2) LVDTs 11 to 14 measured the possible detachment of the masonry infill from the surrounding rc frame; (3) two additional LVDTs were placed to control out-of-plane movement intended to restraint bottom and top rc beams (L15 and L16).

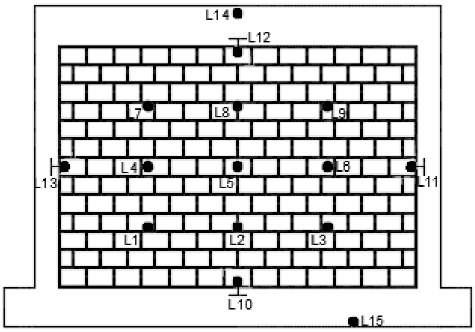

Figure 5. Instrumentation for out-of-plane testing; solid brick infill;

The out-of-plane test was performed under displacement control. In solid brick infill walls the point in which LVDT L5 was attached was selected to control the out-of-plane test, taking into consideration that the maximum displacement of the brick infill panel should occur at this point. In case of brick infill with the central opening, the point at mid span of the lintel above the infill opening, corresponding to LVDT L9, was selected to control the test. In order to implement the displacement control test method, a LabVIEW software was developed to apply a specific pre-defined displacement in the control point of the infill wall.

The displacement-time history for the control point was defined following the recommendations given in FEMA461[12], see Figure 6. The first displacement increment was repeated for six times and the others were repeated two times, enabling to evaluate the stiffness and strength degradation of the masonry infill at each imposed displacement. The displacement increment at each stage *i* was defined as 1.4 times of the displacement at stage *i-1*, following the recommendations given in FEMA461[12] for in-plane quasi-static cyclic loading. Due to the development of plastic deformation in the specimens, the recovery of the total displacement in the unloading branch at the control point was not possible. This means that the real minimum displacement in the unloading process was not zero. However, the Labview software was able to invert the cycles once the residual displacement is attained.

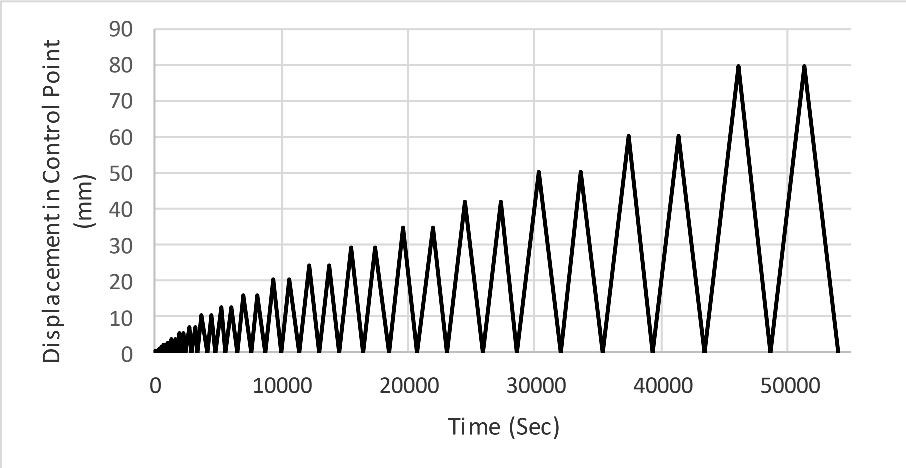

Figure 6. Loading protocol for out-of-plane testing

3 EXPERIMENTAL RESULTS

The main results of the out-of-plane tests are here presented and discussed, including force-displacement diagrams, cracking patterns and deformation contour levels of the different specimens tested.

3.1 Force-displacement diagrams

The force-displacement diagrams obtained for all specimens tested under out-of-plane loading is shown in Figure 7. From the analysis of the force-displacement diagrams obtained for brick masonry infill walls without previous damage it is observed that:

The out-of-plane behavior of brick infills with prior in-plane damage is characterized by lower stiffness and lower out-of-plane strength when compared to sound brick infill (SIF-O-1L-B). In addition, it is seen that the decrease of the lateral stiffness and out-plane strength is higher for specimens with more severe in-plane damage, as expected. In the three specimens with prior damage, the maximum strength is also attained very gradually, being the response of all brick infill walls characterized by a wide pre-peak nonlinear regime. Apart from the lower initial stiffness and strength, the force-displacement diagram of brick infill subjected to in-plane lateral drift equal to 0.3% is rather similar to the behavior exhibited by the sound specimen. The pre-peak regime of brick infills subjected to in-plane lateral drifts equal to 0.5% and 1% is characterized by remarkable change of the stiffness, the envelop being composed of two slopes until the peak strength is attained.

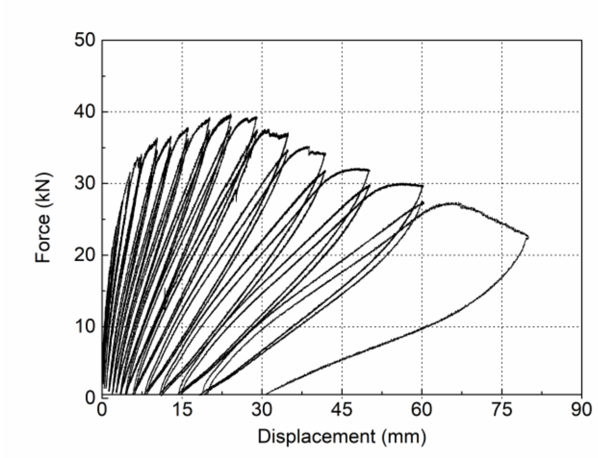

(a)

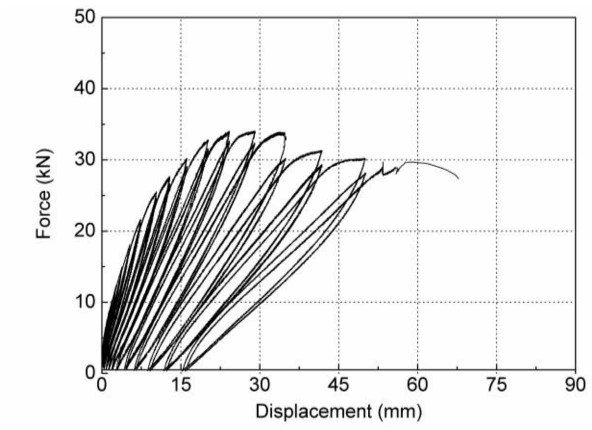

(b)

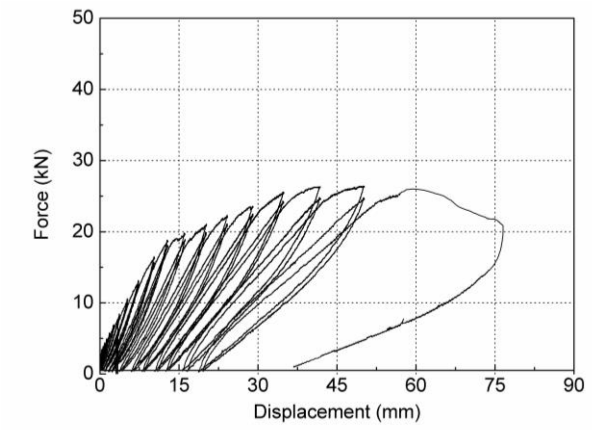

(c)

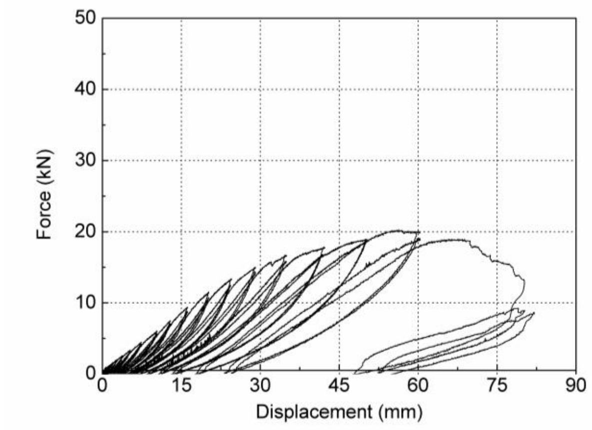

(d)

Figure 7. Force-displacement diagrams of the specimens subjected to out-of-plane loading; (b)SIF-O-1L-B (d)SIF-IO(0.3%)-2L(NC)-B (e)SIF-IO(0.5%)-2L(NC)-B (f)SIF-IO(1%)-2L(NC)-B

3.2 Cracking pattern and out-of-plane deformation

The final cracking pattern and deformation scheme of the rc frames with brick infill tested under out-of-plane loading are shown in Figure 8 and Figure 9. It is observed that the cracking patterns are compatible with the deformation of the masonry infills. It is observed that in the reference specimen, two-way arching mechanism supported on all sides was formed.

In case of specimens with presence of prior in-plane damage, two-way arching mechanism was developed to resist the out-of-plane forces. In the specimen with less prior in-plane damage (SIF-IO(0.3%)-2L(NC)-B), two-way arching mechanism with supports on four sides was developed while in other specimens, due to severe in-plane damage, the upper interface lost its functionality and two-way arching mechanism with supports on three sides was developed. The red lines in the graphs show the cracks that was developed in the in-plane direction. Furthermore, it is clear that the presence of minor in-plane damage does not change the total behavior of the arching mechanism since in both cases (SIF-O-1L-B and SIF-IO(0.3%)-2L(NC)-B) the two-way arching mechanism with supports on all sides was formed.

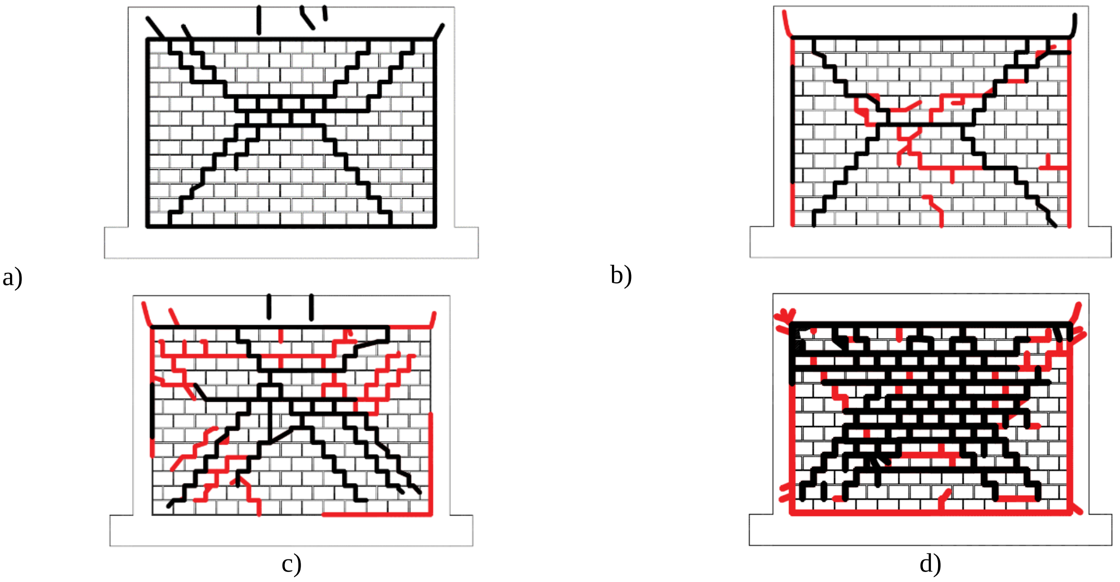

Figure 8. Cracking pattern of the specimens a) SIF-O-1L-B b)SIF-IO(0.3%)-2L(NC)-B c)SIF-IO(0.5%)-2L(NC)-B d)SIF-IO(1%)-2L(NC)-B

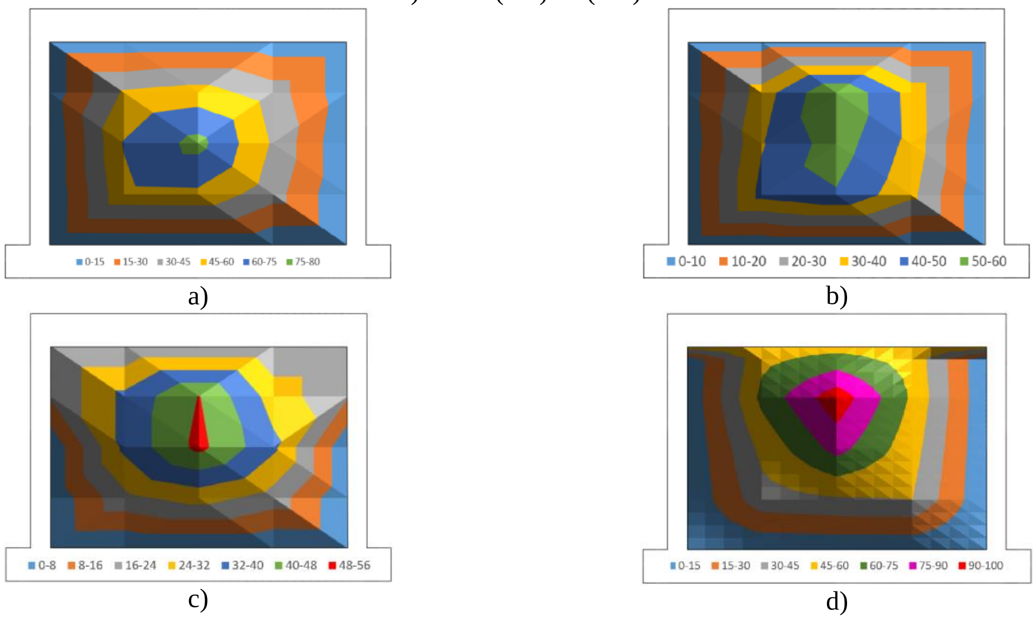

Figure 9. Deformation pattern of the specimens under out-of-plane loading a)SIF-O-1L-B b)SIF-IO(0.3%)-2L(NC)-B c)SIF-IO(0.5%)-2L(NC)-B d)SIF-IO(1%)-2L(NC)-B

During the out-of-plane tests it is observed that in the specimen with minor in-plane damage, the cracking pattern at low levels of out-of-plane loading is affected by the prior in-plane damage, but at higher levels of loading its influence is reduced and new cracks were developed. Inclusively, the cracking observed at the right vertical interface did not evolve in the out-of-plane loading. For specimens with severe in-plane damage (SIF-IO(0.5%)-2L(NC)-B and SIF-IO(1%)-2L(NC)-B), the out-of-plane cracking of the specimens were totally influenced by prior in-plane cracks even in the low or high levels of out-of-plane loading.

4 EVALUATION OF OUT-OF-PLANE PERFORMANCE

The out-of-plane performance of the reinforced concrete frames with masonry infills was discussed based on different parameters, namely: (1) the influence of prior in-plane damage (2) construction quality (3) presence of openings and (4) energy dissipation capacity.

4.1 Effect of prior in-plane damage on the out-of-plane response

The out-of-plane force-displacement monotonic envelopes of specimen (SIF-O-1L-B) is compared with monotonic envelopes of specimens with different levels of previous in-plane damage in Figure 10. Besides the clear reduction of the out-of-plane strength, there is also a great variation on the out-of-plane stiffness.

The main quantitative parameters taken from these envelopes, namely initial stiffness, secant stiffness at 30% of the maximum out-of-plane force and out-of-plane resistance are presented in Table 3. It is clear that the prior in-plane damage reduces both the stiffness (initial or secant stiffness at 30% of the maximum out-of-plane force) and the lateral strength of the masonry infilled frames. The reduction level depends on the severity of the damage induced by prior in-plane loading. The out-of-plane strength of the specimen with severe in-plane damage (SIF-IO(1%)-2L(NC)-B) is half of the out-of-plane strength of the specimen without prior in-plane damage. The values for the initial and secant stiffness on this specimen is about 10% and 5% of the initial and secant stiffness measured in the reference specimen without prior in-plane damage. This emphasizes that the influence of the prior in-plane damage on stiffness is rather high.

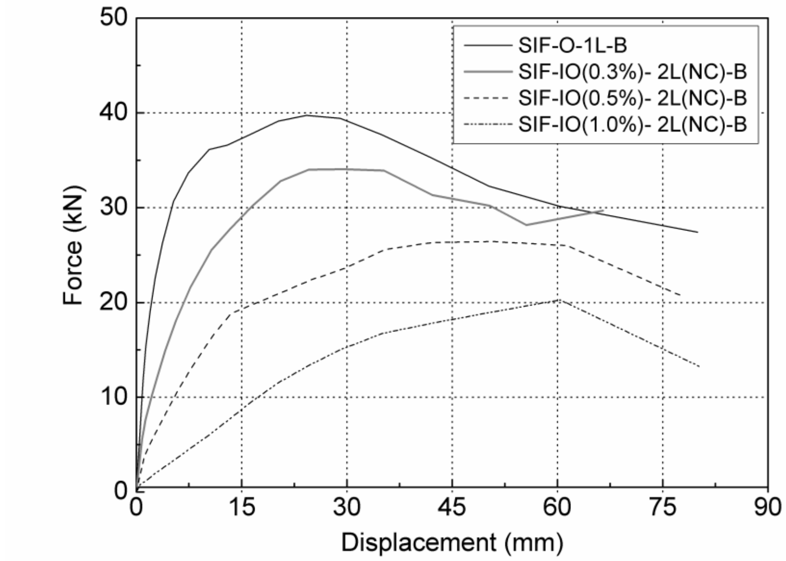

Figure 10. Out-of-plane force-displacement monotonic envelops of specimens constructed with mason type B

Model	Initial Stiffness (kN/mm)	Secant Initial Stiffness (kN/mm)	Out-of-plane strength (kN)
SIF-O-1L-B	12.5	12.5	39.8
SIF-IO(0.3%)-2L(NC)-B	6.8	4.9	34.0
SIF-IO(0.5%)-2L(NC)-B	3.4	2.0	26.4
SIF-IO(1%)-2L(NC)-B	1.3	0.58	20.3

Table 3. Secant stiffness and out-of-plane strength of different specimens built with mason type B

The variation of the normalized secant stiffness calculated at 30% of the peak force and of normalized out-of-plane strength found for the specimens with prior in-plane damage with respect to lateral in-plane drift are shown in Figure 11. It is observed that the stiffness of the masonry infills with prior in-plane damage decreases exponentially by increasing imposed lateral drift to the levels of 0.3%, 0.5% and 1%. The experimental values are well fitted by an exponential function with a coefficient of correlation equal to 0.99. This seems to indicate that the reduction rate for lower values of prior in-plane drift is high.

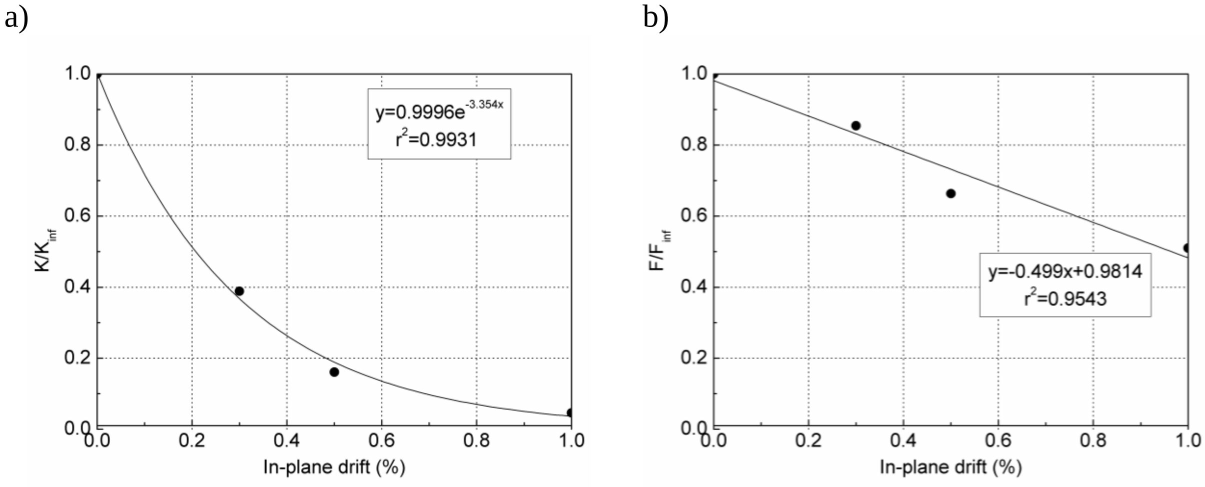

Figure 11. Variation of a)initial stiffness and b)out-of-plane strength with respect to prior in-plane drift

The out-of-plane strength presents a linear decreasing variation as the in-plane damage increases. The linear trend fitted to the experimental results presents a very reasonable coefficient of variation (R^2=0.95), see Figure 11b. The masonry infill with prior in-plane damage corresponding to in-plane drift of 1% could withstand 50% of the out-of-plane strength of the specimen with no prior in-plane damage.

Based on the analytical trends obtained from the fitting to the experimental results (Figure 12), it is possible to obtain expressions for estimation of stiffness and out-of-plane resistance of masonry infills with prior in-plane damage. Therefore, the variation of the secant stiffness of damaged specimens can be estimated as:

$$K = K_{\inf}(e^{-3.3D}) \tag{1}$$

Where K (kN/mm) is the out-of-plane secant stiffness of the masonry infill subjected to prior in-plane drift of D(%) and K_{inf} (kN/mm) is the out-of-plane secant stiffness of the specimen without previous in-plane damage.

Similarly, the out-of-plane strength, F (kN), of the masonry infills subjected to prior in-plane drift of D (%) can be estimated based on the strength of undamaged infill, F_{inf} (kN), and taking into account the level of prior in-plane drift, through the following equation:

$$F = F_{\inf}\left(\frac{2-D}{2}\right) \tag{2}$$

The values of the predicted stiffness and out-of-plane strength obtained by these simplified equations are presented in Table 4 and compared with the experimental results. It is observed that the developed equations can satisfactorily predict the reduction of the secant stiffness and out-of-plane strength of the infilled frames due to presence of prior in-plane damage. The highest error in the prediction of stiffness was found for specimen SIF-IO(1%)-2L(NC)-B, but this is mainly attributed to the low values of stiffness.

Notice that the values of secant stiffness were always calculated following the same procedure by considering the slope of the line connecting the origin to the point with 30% of the out-of-plane strength. However, it should be mentioned that the specimens were already cracked due to in-plane loading, resulting in an expected reduction on the secant stiffness in the out-of-plane direction. Therefore, if instead of considering the secant stiffness at 30% of the lateral strength the initial stiffness is calculated, the stiffness reduction trend can be represented by the exponential curve shown in Figure 12.

Specimen	K/K_{inf}			F/F_{inf}		
	Experiment	Simplified equation	Error (%)	Experiment	Simplified equation	Error (%)
SIF-O-1L-B	1.00	1.00	0.0	1.00	1	0.0
SIF-IO(0.3%)-2L(NC)-B	0.39	0.37	-5.1	0.85	0.85	0.0
SIF-IO(0.5%)-2L(NC)-B	0.16	0.19	-18.8	0.66	0.75	13.6
SIF-IO(1%)-2L(NC)-B	0.05	0.04	20.0	0.51	0.5	-2.0

Table 4. Comparison between experimental and analytical results

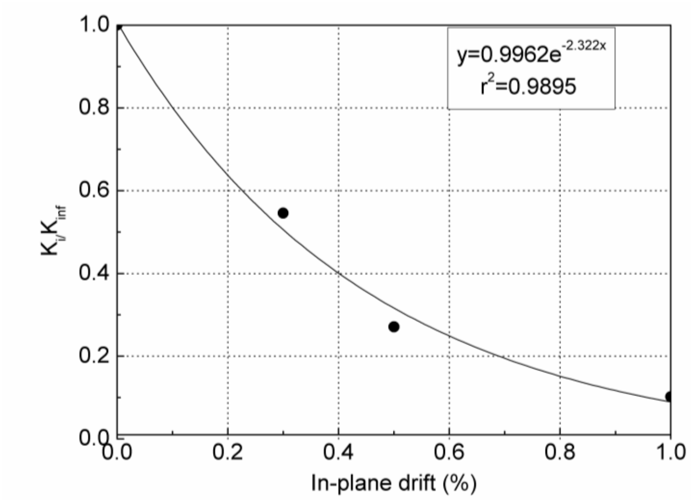

Figure 12. Variation of the initial stiffness of the specimens with respect to prior in-plane damage

It is clear that the trend of variation of the initial stiffness is also similar to an exponential curve and can be estimated as:

$$K^{in} = K^{in}_{\text{inf}}(e^{-2.4D}) \qquad (3)$$

Where K^{in} (kN/mm) is the out-of-plane initial stiffness of the masonry infill subjected to prior in-plane drift D(%) and K^{in}_{inf} (kN/mm) is the out-of-plane initial stiffness of the specimen without previous in-plane damage. The values of the predicted initial stiffness of the specimens were compared with experimental results, see Table 5. It is clear that eq. 3 can satisfactorily predict the initial stiffness of the damaged specimens.

Specimen	K/K_{inf}		
	Experiment	Simplified equation	Error (%)
SIF-O-1L-B	1.00	1.00	0.0
SIF-IO(0.3%)-2L(NC)-B	0.55	0.49	10.9
SIF-IO(0.5%)-2L(NC)-B	0.27	0.30	-11.1
SIF-IO(1%)-2L(NC)-B	0.10	0.09	10.0

Table 5. Comparison between experimental and analytical results

The stiffness degradation curves of masonry infills with different levels of previous in-plane damage are shown in Figure 13. It is clear that the specimens with lower amount of prior in-plane damage exhibited higher initial out-of-plane stiffness. Looking at those graphs in Figure 13, it is clear that the initial out-of-plane stiffness of the specimens with less in-plane damage degraded with higher rate than the specimens with severe in-plane damage.

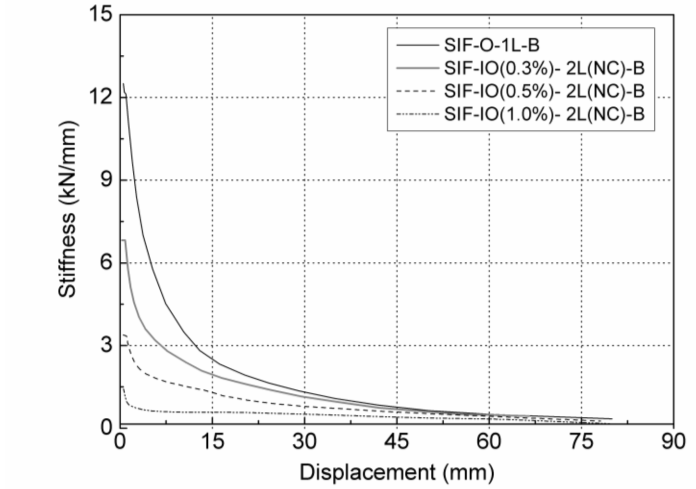

Figure 13. Stiffness degradation curve of the specimens constructed by mason B

4.2 Energy dissipation capacity

The cumulative energy dissipated until a certain lateral drift obtained in masonry infills with different levels of previous in-plane damage is shown in Figure 14. The comparison of the cumulative dissipated energy between the reference solid specimen built by mason B with the specimen constructed by mason A and specimen with central opening is presented in Figure 15. The influence of prior in-plane damage on the variation of cumulative dissipation of energy is clearly revealed by the decreasing of the energy dissipated in damaged brick infills with respect to the reference brick masonry infill. In addition, it is seen that the dissipated energy is decreasing as the damage level increases. This is mainly justified by the presence of previously opened cracks during in-plane tests. In fact, part of the cracks that was developed during in-plane tests, open again during the out-of-plane tests but the energy needed for its opening is much lower, when compared to the energy needed to open new cracks. This means that more reduced energy is needed to re-open the cracks, in opposite to the energy needed to open new cracks.

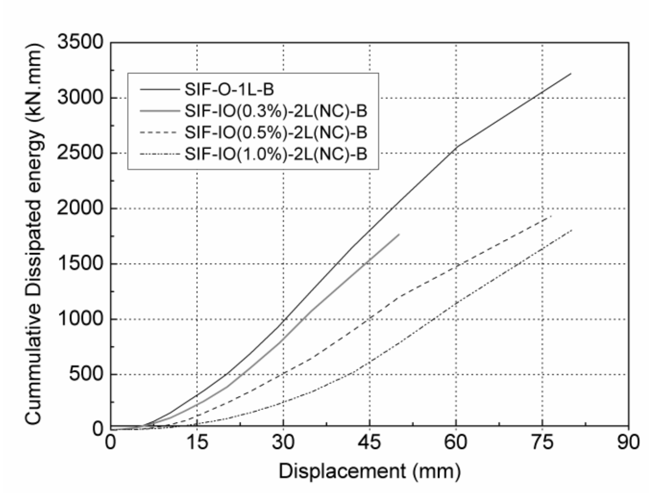

Figure 14. Total dissipated energy of specimens with different prior in-plane damage

From Figure 15, it is seen that the brick infill with central opening (PIF-O-1L-B) exhibit similar trend but slightly higher values of dissipated energy than the specimen with solid brick infill (SIF-O-1L-B) until out-of-plane displacement of 25mm, corresponding to the maximum out-of-plane displacement of the brick infill with the central opening. The higher total amount of energy dissipated in the solid brick infill is attributed to the much higher deformation capacity. The same trend was observed in the brick infill built by mason A until the out-of-plane displacement of 30mm.

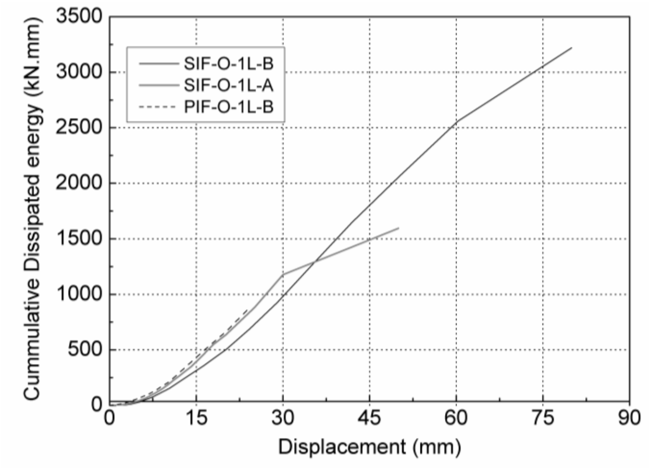

Figure 15. Total dissipated energy of specimens constructed by different masons and with central opening

5 CONCLUSIONS

This paper presented and discussed the results of an experimental campaign carried out on traditional brick masonry infills of south European countries under out-of-plane loading simulated through an airbag. The influence of previous in-plane damage in the out-of-plane performance was analyzed. From the results obtained, the following conclusion can be drawn:

- the initial stiffness of specimens varies exponentially with respect to the level of prior in-plane drift. This means that severe prior in-plane damage leads to lower initial stiffness.
- The residual deformation of brick walls, which is more relevant after its cracking, increases with the progress of damage in the masonry infill.
- Prior in-plane damage results in decreasing of the out-of-plane initial stiffness and out-of-plane strength. The previous in-plane damage also influences the cracking and deformation patterns, mainly due to the previous in-plane cracks and collapse of the upper interface between brick infill and rc concrete beam.
- The initial out-of-plane stiffness of brick walls subjected to previous in-plane damage can be estimated through an exponential function taking into account the initial stiffness of brick masonry infill without damage and taking advantage of the damage index.
- The out-of-plane strength of brick walls subjected to previous in-plane damage can be estimated through a linear function using the out-of-plane strength of brick masonry infill without damage and taking advantage of the damage index.

- The energy dissipation capacity of the solid brick wall without an in-plane damage is significantly higher than the energy dissipation capacity of the specimens that have prior in-plane damage.

REFERENCES

[1] Braga F, Manfredi V, Masi A, Salvatori A, Vona M. Performance of non-structural elements in RC buildings during the L'Aquila, 2009 earthquake. Bull Earthquake Eng. 2011;9:307-24.

[2] Drysdale R, Essawy A. Out‐of‐Plane Bending of Concrete Block Walls. Journal of Structural Engineering. 1988;114:121-33.

[3] Tu Y-H, Chuang T-H, Liu P-M, Yang Y-S. Out-of-plane shaking table tests on unreinforced masonry panels in RC frames. Engineering Structures. 2010;32:3925-35.

[4] Flanagan R, Bennett R. Bidirectional Behavior of Structural Clay Tile Infilled Frames. Journal of Structural Engineering. 1999;125:236-44.

[5] Dazio A. Effect of boundary conditions on the out-of-plane behavior of unreinforced masonry walls. 14th World Conference on Earthquake Engineering. Beijing, China2008.

[6] Dafnis A, Kolsch H, Reimerdes H. Arching in Masonry Walls Subjected to Earthquake Motions. Journal of Structural Engineering. 2002;128:153-9.

[7] Dawe JL, Seah CK. Out-of-plane resistance of concrete masonry infilled panels. Canadian Journal of Civil Engineering. 1989;16:854-64.

[8] Akhoundi F, Lourenço PB, Vasconcelos G. Numerically based proposals for the stiffness and strength of masonry infills with openings in reinforced concrete frames. Earthquake Engineering & Structural Dynamics. 2016;45:869-91.

[9] Angel R, Abrams D, Shapiro D, Uzarski J, Webster M. Behaviour of reinforced concrete frames with masonry infills. Urbana-Champaign, IL, USA, 1994.

[10] Furtado A, Costa C, Rodrigues H, Arêde A. Characterization of structural characteristics of Portuguese buildings with masonry infill walls stock. 9th International Masonry Conference. University of Minho, Guimarães , Portugal2014.

[11] ACI318-08. Building Code Requirements for Structural Concrete (ACI 318-08) and Commentary. American Concrete Institute; 2008.

[12] FEMA461. Interim Testing Protocols for Determining the Seismic Performance Characteristics of Structural and Nonstructural Components. Washington, D.C.: FEDERAL EMERGENCY MANAGEMENT AGENCY; 2007.